JOURNAL OF MATERIALS SCIENCE 37 (2002) 989–995

Quantification of the recrystallization behaviour in Al-alloy AA1050

S. P. CHEN, D. N. HANLON, S. VAN DER ZWAAG
Lab. for Materials Science, Netherlands Institute for Metals Research, TU Delft Rotterdamseweg 137, 2628AL, Delft, The Netherlands
E-mail: s.vanderzwaag@stm.tudelft.nl

Y. T. PEI, J. TH. M. DEHOSSON
Department of Applied Physics, Materials Science Center and Netherlands Institute for Metals Research, University of Groningen, Nijenborgh 4, 9747 AG Groningen, The Netherlands

A new methodology for the determination of the recrystallized volume fraction from anodically etched aluminium alloys using optical microscopy is described. The method involves the creation of a composite image from multiple micrographs taken at a series of orientations. The results of quantitative analysis of images obtained by this new method are compared with those obtained using the traditional single image optical microscopy technique, orientation imaging microscopy (OIM) and microhardness indentation. The multiple orientation image method is shown to consistently yield a recrystallized volume fraction which is significantly higher than that determined from a single image while multiple orientation imaging and OIM results are found to be in good agreement. Furthermore it is shown that, after the subtraction of the effect of concurrent recovery using the rule of mixtures, microhardness indentation can also be used to determine the recrystallized volume fraction.

1. Introduction

In any study of the kinetics of recrystallization, it is important to determine the volume fraction of recrystallized material as accurately as possible. Several techniques are currently in use to quantify the recrystallization behaviour of deformed metals. The most widely used method is that of optical microscopy performed on a series of samples recrystallized to different extents [1–4]. In addition to yielding quantitative information regarding the extent of recrystallization, this technique provides some insight into other microstructural features such as grain size as well as patterns of nucleation and growth. However, when this method is applied to aluminium alloys such as AA1050, it turns out to be rather difficult to obtain precise data on the recrystallized fraction. Traditionally, an anodic etching technique is used to reveal the grain structure and a number of micrographs are taken of randomly selected areas. A point-counting technique is then applied to obtain average values of the recrystallized fraction [1, 3]. However, when observed directly at a single orientation with respect to the polarisors the grain structure of a partially recrystallized aluminium sample prepared in this manner is rarely clearly and unambiguously visible in its entirety [5]. When the sample is rotated under polarized light, the microstructure in a field of view seemingly undergoes a metamorphosis in which apparently unrecrystallized regions begin to appear recrystallized (as previously hidden boundaries become visible) and apparently recrystallized regions begin to appear unrecrystallized (as internal substructural details become visible). This situation leads to extra complications in the identification of recrystallized grains with only a single micrograph. In order to eliminate such uncertainties in the determination of the fraction recrystallized, in this paper, a new method has been designed which is based on the construction of a composite image of a single region produced from a set of single micrographs taken at a series of stage rotations. This method enables the structure to be faithfully revealed and thus enables the recrystallized fraction to be more accurately determined.

Recently, orientation imaging microscopy (OIM) has been employed to determine the recrystallized fraction [6–9] in Al-base alloys. Although so far OIM has been predominately applied to the determination of texture, grain boundary structure and phase determination, an important potential application of OIM lies in the field of recrystallization, in particular the determination of recrystallization kinetics and the crystallographic relationships between recrystallized and unrecrystallized grains. By OIM, it is possible to determine accurately whether an area is recrystallized. Other, indirect methods (hardness indentations, x-ray diffraction, neutron diffraction and electrical resistivity) have also been employed [1, 10–12] to determine the recrystallization fraction. These methods measure certain effects of micostructural changes on the properties and provide only average values including both recovery and recrystallization effects. Nevertheless, if

the effects of recovery and recrystallization can be separated such techniques may provide valuable additional information regarding recrystallization behaviour. In this study OIM and microhardness measurement have been employed along with the optical microscopy techniques described above to determine the recrystallization fraction in the commercially pure AA1050 alloy. The results so obtained are compared and critically discussed.

2. Experimental details

2.1. Material preparation

The chemical composition of the commercially pure aluminium alloy AA 1050 used is: 0.185 wt% Fe, 0.109 wt% Si and Al in balance. The material contains plate-shaped intermetallic compounds $FeAl_3$, which have an aspect ratio in the range of 1 to 6. The size of $FeAl_3$ particles ranges between 0.2 and 7 μm.

In order to produce material in a suitable form for further experimentation a cast ingot of AA1050 was hot rolled in 19 passes, resulting in a reduction in thickness from 500 mm to 4 mm. The hot rolling processes started at 520°C and finished at 305°C. The hot-rolled material was annealed at 600°C for 2 h and then quenched into water. The material was again heated to 400°C and held at this temperature for 2 h to reduce the content of iron in solid solution. The average grain size after this treatment was 90 μm.

The materials were finally cold rolled to a reduction in thickness of 50% (from 4 mm to 2 mm). The rolled sheet was cut into small samples of $20 \times 15 \times 2$ mm. The samples were annealed in a salt bath at 340°C for times ranging from 30 s to 3 h and then quenched into water to obtain different extents of recrystallization. The temperature of the salt bath was controlled to within an accuracy of ± 2°C. The time taken for a specimen to reach the set temperature was approximately 5 seconds.

2.2. Microstructural characterization

The optical microscopy and OIM as well as microhardness examinations were carried out on the section parallel to the RN plane (R rolling direction and N surface normal) to encounter as many grain boundaries as possible. After standard sectioning and polishing, specimens for optical metallography were etched anodically with Baker's reagent (1% HBF_4 aqueous solution) [13] at 20 V for approximately 120 s depending on the annealing time. For OIM scanning, the specimens were etched with Keller's reagent for 30 seconds. In order to account for inhomogeneities in the microstructure in the through thickness direction of the sheet, all the metallography and hardness measurements were performed at locations along the center line of the sheet, in a band covering approximately one third of the thickness of the sheet.

The optical microscopy examinations were performed using a NEOPHOT inverted stage metallurgical microscope. Both a standard point-counting technique and a LEICA QUANTIMET digital image analysis facility were used to evaluate the recrystallized fraction. In all cases measurements were conducted on five separate areas.

Orientation imaging microscopy (OIM), developed by TexSEM Laboratories Inc., was integrated with a Philips XL-30s FEG scanning electron microscope (SEM) and employed for the combined microstructural and crystallographic analysis. By a fast procedure of capturing and processing electron back-scatter diffraction patterns (EBSPs), the OIM system produces thousands of orientation measurements, linking local lattice orientation with grain morphology. Each measurement is represented by a pixel in the orientation micrographs, to which a colour or grey scale value is assigned on the basis of the local details of lattice orientation or the quality of the corresponding EBSP image quality (IQ). Recrystallized grains are distinguished according to IQ and orientation spread. The volume fraction of recrystallized material was determined from the ratio of the area of the recrystallized grains to the area of the whole image. In this work the area of a typical OIM scan was about 1800×600 μm^2, containing approximately 130 deformed grains.

A Buehler OMNIMET MHT automatic micro hardness tester was used for the microhardness measurements. The micro hardness of each specimen was determined, using 50 g load and 15 s loading time. Hardness tests were made after polishing and 18 measurements were taken on each specimen.

2.3. Composite image method

In order to construct composite images a total of four micrographs at 20° stage rotation intervals were taken from each area. The rotation centre of the stage should be aligned perfectly with the objective lens so that no misalignment of the micrographs results. The following step was to trace all visible recrystallized grains from each of the micrographs onto an acetate sheet in order to construct a single representation containing all recrystallized regions. To reveal the contribution to the total volume fraction made by each rotation, a separate colour was used to trace the visible recrystallized structure from each individual micrograph. The border of each micrograph was also traced in order to define a common overlaid area. Quantitative metallography (a standard point counting technique) was then performed using the composite image. In this study the criteria used to determine whether a grain is recrystallized were the following:

1. Size: Grains with an area considerably smaller (<10%) than the original deformed average grains were taken to be potentially recrystallized grains (when the fraction recrystallized is small).
2. Polygonality: Polygonal grains with sharp triple points and straight boundary edges were viewed as potentially recrystallized grains.
3. Equiaxiallity: Grains with low aspect ratios were taken to be potentially recrystallized grains. In this study those grains having an arbitrarily chosen aspect ratio up to and including 1.75 are considered to be recrystallized, the reminder being classed as unrecrystallized.

4. Absence of a visible internal structure: Absence of deformation bands was taken as an additional indication of recrystallized grain character.

A further development of the technique is to use colour micrographs in an attempt to reduce the apparent metamorphosis. By adding a 1/4 λ filter, grains with different orientation will exhibit different colours under polarized light. This facilitates a better identification of the recrystallized grains. In this investigation, similar composite images were composed from colour digital micrographs according to the procedure described above. The unrecrystallized material can be extracted from the digital image. The fraction of the recrystallized area, the recrystallized grain sizes (defined as square root of grain area divided by $\pi/4$) of individual grains and grain size distribution were then calculated using automated areal analysis.

3. Results

3.1. Microstructural evolution

The deformed structures show that the grains in the central part of the rolled sheet follow the same shape change as the whole specimen. The grains are elongated in the rolling direction and exhibit a pancake shape with a thickness of 45 μm on average, i.e. half of the initial grain size. The triple point angles among the grains are distorted and not equal to 120°. The as-deformed grain structure showed non-uniform colours within the grains and somewhat unclear grain boundaries. The non-uniform colours reflect the local variation in the disturbance of the crystal created during deformation.

After annealing the deformed sheet at 340°C for 5 minutes, the triple point angles tend to return towards 120°. Few nuclei were observed at the pre-existing grain corners and along the grain boundaries. The newly formed recrystallized grains exhibited a uniform colour within the grains and sharp grain boundaries. There are some indications of strain-induced migration of pre-existing grain boundaries (SIBM). As the annealing time increases to 10 min, the pre-existing grain boundaries became corrugated. More nuclei can be seen at the pre-existing grain corners or along the gain boundaries. Clusters of nuclei can be observed. Fig. 1 shows the nuclei along the boundaries of the pre-existing deformed grains and the SIBM in regions close to grain edges. After 20 minute annealing, evidence of strain-induced migration of pre-existing grain boundaries is obvious. The number of nuclei is still increasing and at the same time nuclei coalescence is observed. Some of the deformed grains were found to have many more nuclei than others whilst some of them were still nuclei free. When annealed for 30 minutes or longer, the density of the nuclei remained constant. However, the size of the recrystallized grains increases with annealing time. No nuclei were found around $FeAl_3$ particles.

3.2. Composite imaging analysis

Fig. 2 shows a series of colour micrographs taken at 20° rotation intervals of a sample after annealing 50 min at 340°C. As can be seen, the area labelled A in Fig. 2a

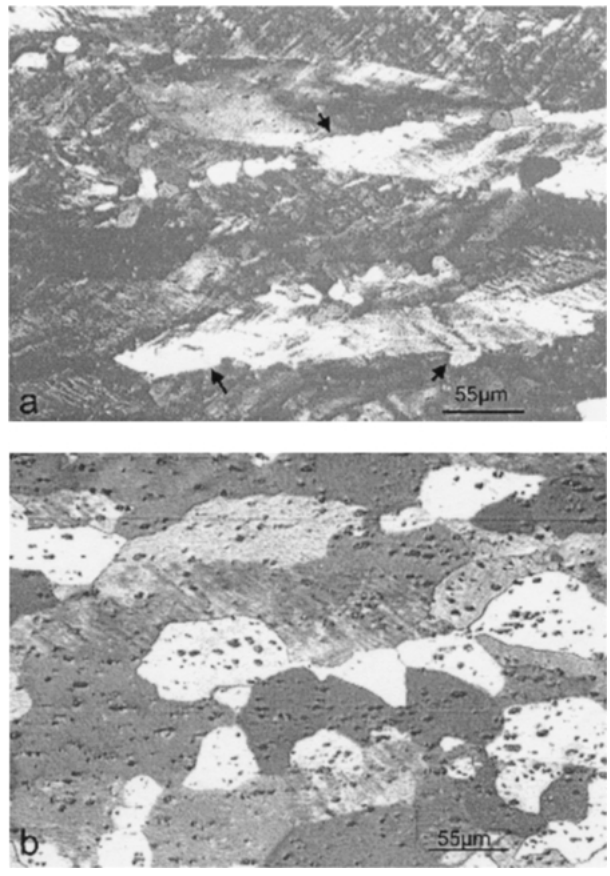

Figure 1 Optical micrographs showing the microstructure of AA 1050 recrystallized at 340°C for (a) 10 min and (b) 60 min. Arrows indicate the SIBM of region close to the pre-existing grain boundaries.

seems to be one grain but it is clear in Fig. 2b and c that it actually consists of two grains. One may easily identify the grain boundary at position B on Fig. 2b and c, but it is hardly visible in Fig. 2a. The difference in the individual micrographs is a clear illustration that it is difficult to determine an accurate recrystallized fraction from a single micrograph.

The area fractions recrystallized obtained from single and composite images using the point counting technique are displayed in Fig. 3. It can be seen that consideration of a single image leads to a significant underestimate of the volume fraction of recrystallized material. For all the samples studied the composite images constructed from three orientated micrographs yield a volume fraction about 50% higher than estimated from a single micrograph. For the samples under investigation here, more than three micrographs do not show a significant modification to the composite images and consequently do not lead to a further increase of the measured fraction. The points represent the mean values, and the error bars (shown only for the measurements on the composite images composed from three micrographs) indicate the spread of the individual measurements.

Fig. 4 shows a histogram of the recrystallized grain size at various times obtained by composite images combined with the automated areal analysis technique. It seems that the recrystallized grain sizes in the partly recrystallized material follow an approximately log-normal distribution. The maximum equivalent diameter of the recrystallized grain, d_{max}, and the mean grain size, d_{mean}, are employed to describe

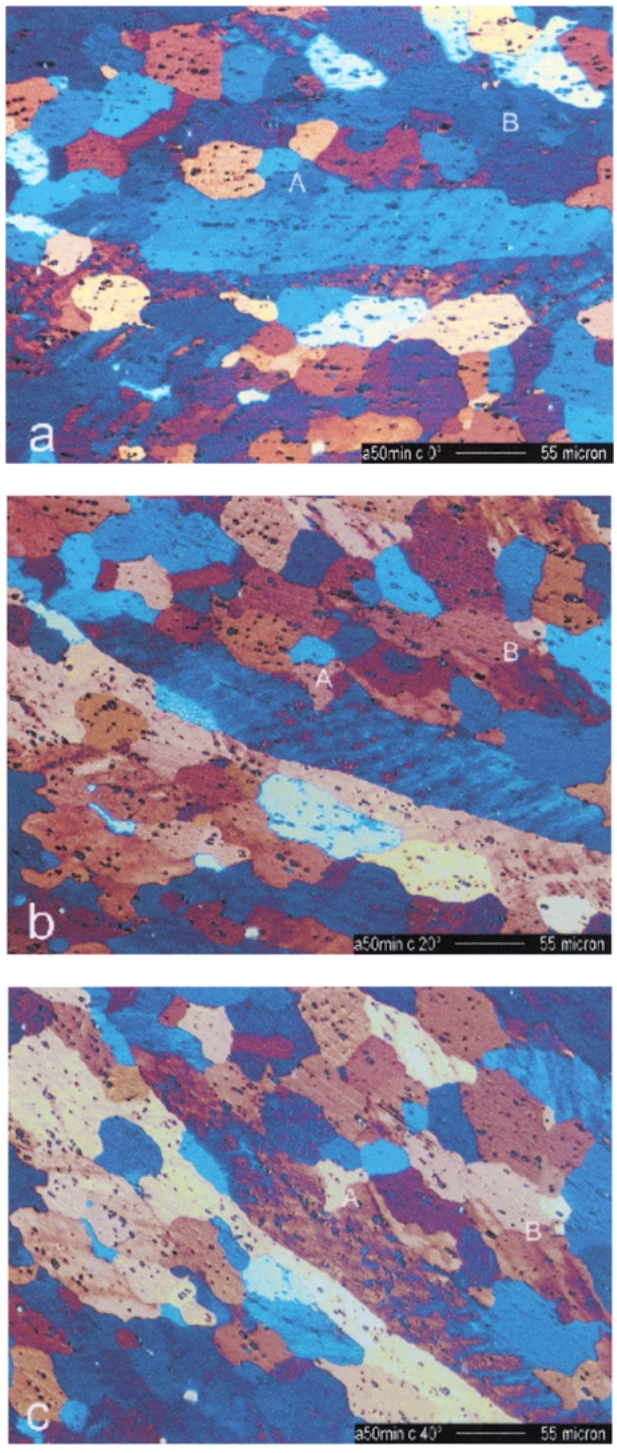

Figure 2 Multiple micrographs showing the microstructural metamorphosis at locations A and B when rotating the sample annealed at 340°C for 50 min.

the grain size evolution, which is shown in Fig. 4d. Both curves demonstrate that the growth rate of the recrystallized grains decreases with annealing time and the difference between the two curves becomes larger. As can be seen in Fig. 1, the impingement between the clustered grains may prevent them from growing further. This explains the big difference between d_{max} and d_{mean} at the later stage of recrystallization.

3.3. OIM observation

Fig. 5 shows an OIM image of the same sample as in Fig. 2. The left part in Fig. 5 is the same region as in

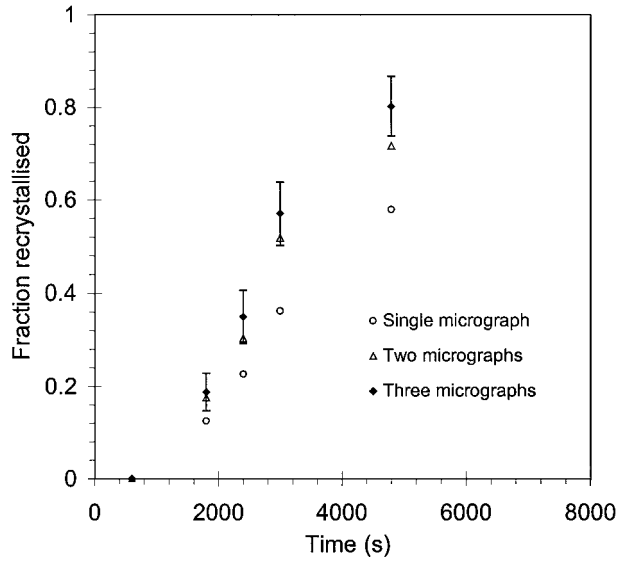

Figure 3 Recrystallization fraction determined on single and composite images by point counting technique, showing the effect of multiple orientated micrographs.

Fig. 2 in which there is a nearly perfect grain match with the conventional microstructure (a mirror image). The black lines indicate high angle grain boundaries with a misorientation larger than 15°, and the thin blue and gray lines in a deformed grain represent sub-grain boundaries with a misorientation angle between 10–15° and 4–10°, respectively. From the combined information of Inverse Pole Figure (IPF) maps and IQ maps, recrystallized grains can easily be distinguished from non-recrystallized grains. The recrystallized grains are uniform in colour, which means that the spread in orientation within the grains is quite small, and free from low angle sub-grain boundaries. In contrast, the non-recrystallized grains contain deformation substructures as revealed in slightly different colours and low angle sub-gain boundaries. Correspondingly, the recrystallized grains are much brighter than the non-recrystallized grains on the IQ map. This is indicative of a high degree of crystal perfection.

Fig. 6 shows the recrystallized fraction determined from OIM for several annealing times. The results obtained with the optical microscopy technique (the manual point counting and automated area analysis) are also shown for comparison. Here the attached error bars are only shown for area analysis (error is within ±5%). The values from the point counting technique are lower than those from the areal analysis and both results are slightly lower than the data from OIM but still within the experimental scatter of areal analysis data.

3.4. Micro-hardness measurements

The micro hardness (HV) measurements after isothermal annealing at 340°C for various times are shown in Fig. 7a on log time scale. From the error bars it can be seen that there is a large scatter between the individual hardness measurements. However, an overall clear pattern of annealing behaviour can be observed. Similar to the optical microscopy determination, the sizes of the error bars are larger in the intermediate

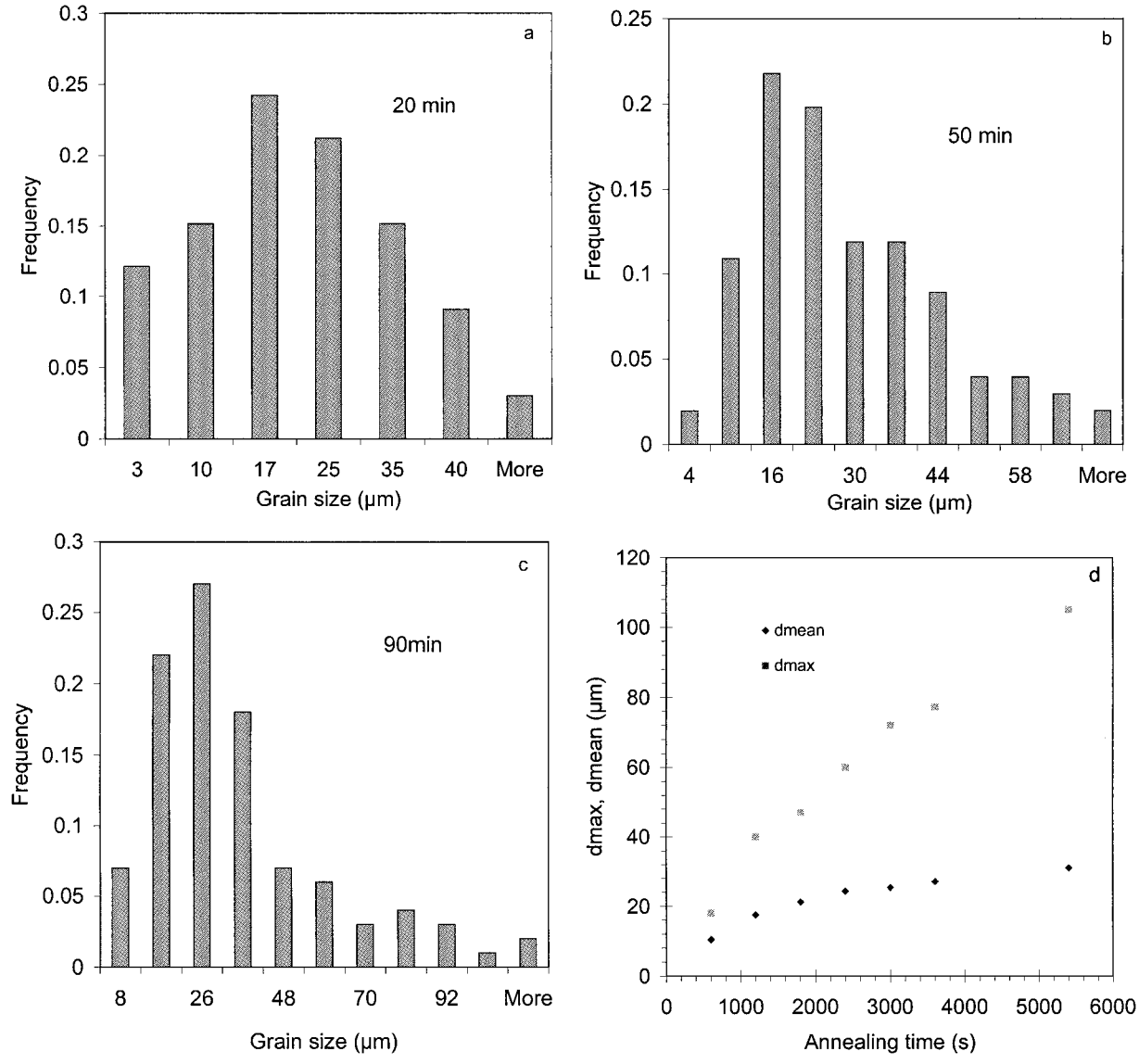

Figure 4 Size evolution of recrystallized grains vs annealing time.

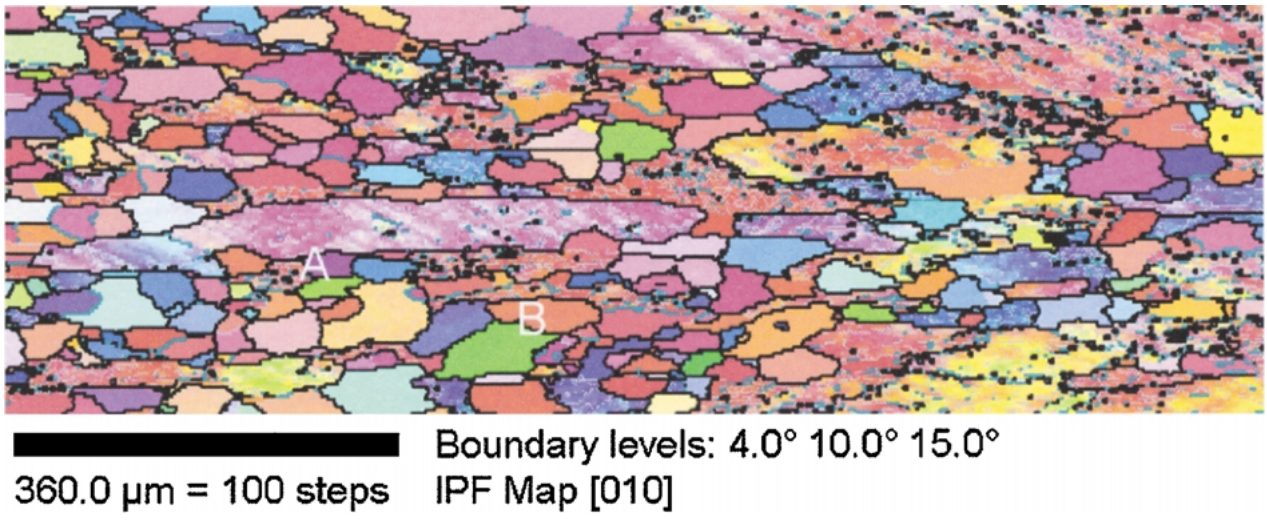

Figure 5 OIM map (IPF) showing the microstructure and boundaries with different misorientation levels in the same sample as in Fig. 2.

time range, which demonstrates the inhomogeneous character of the partially recrystallized material. It can be seen that the hardness curve from the onset of annealing to the point that represents 2% recrystallized material (according to optical microscopy examination) can be represented by a straight line. The slope of the curve increases when the recrystallization process starts. It indicates a rapid decrease of hardness with increasing faction of recrystallized material. The microhardness of a sample directly after cold work (H_m) is 46.8 and

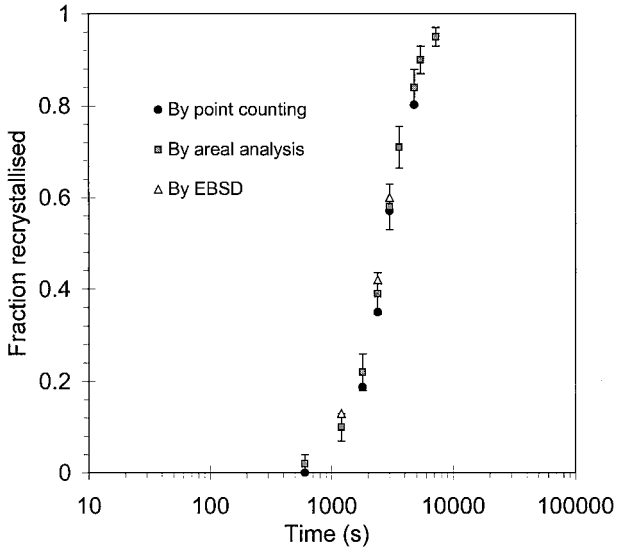

Figure 6 Comparison of the fraction of recrystallized material determined by composite image method and by OIM.

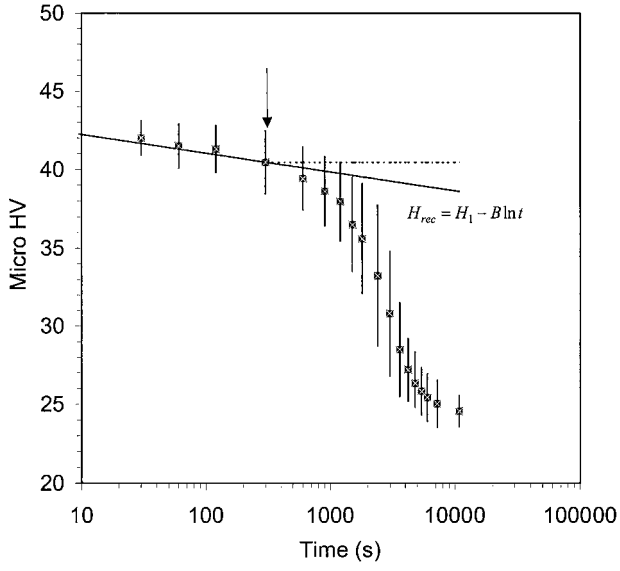

(a)

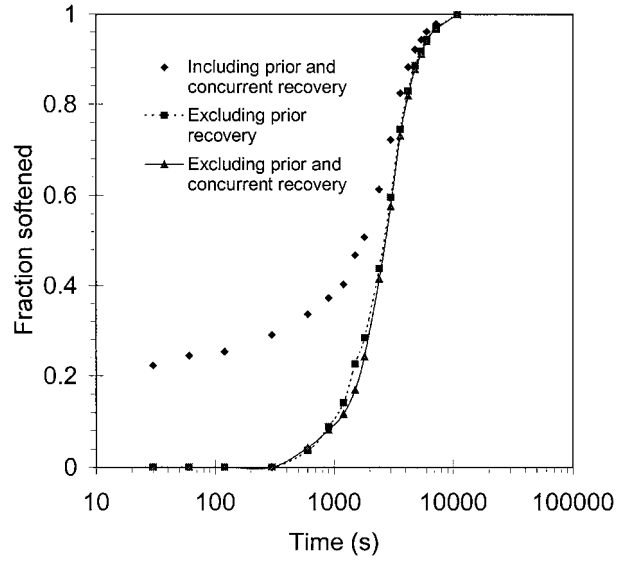

(b)

Figure 7 Microhardness measurements (a) and the derived fraction of recrystallized material after subtraction of recovery effects (b).

that of the fully recrystallized material (H_0) is 24.5. The softening fraction, R, of an annealed sample could be calculated from these two values as follows [1, 14]

$$R = \frac{H_m - H}{H_m - H_0} \quad (1)$$

Where H the measured hardness. R calculated according to formula (1) is plotted in Fig. 7b (diamond symbol). Obviously this data includes the softening effect contributed by both recovery and recrystallization, as will be discussed later.

4. Discussion

4.1. Composite image method

The work was aimed at accurately quantifying the fraction of recrystallized material using optical microscopy. As demonstrated in Fig. 2, taking only a single image can not provide complete information of the partially recrystallized microstructure. If two neighbouring grains are oriented in such a way that certain lattice planes of both lie roughly perpendicular to the direction of the polarized light, they will exhibit a similar colour. Therefore, some recrystallized grains may not be distinguished from the deformed parent grain in a single micrograph. As a result, the measured fraction may be underestimated. Here it is shown that this problem can be easily overcome by using composite micrographs produced by repeatedly rotating the sample (by e.g. 20°) around the optical axis. The grain boundaries that are not shown in a single micrograph can be revealed in others. By this new method the characterization of recrystallized grains is more reliable and a more accurate recrystallization fraction is obtained.

4.2. Comparison of optical and OIM techniques

The fractions of recrystallized material determined by optical microscopy (multiple orientation images combined with manual point counting and automated area analysis) and by OIM show an excellent agreement. Both techniques show the same course of transformation. Measurements by OIM yield slightly higher values of the fraction, especially at shorter annealing times.

Because of the resolution limit, the smallest recrystallized grain size that can be clearly observed by the optical microscopy under polarized light is of the order of 2–5 μm. Therefore, the results obtained in this way only reflect the recrystallization behaviour. Recovery will not affect the results obtained by OIM, as (1) recovered regions still contain fairly small subgrains; (2) no significant lattice reorientation occurs (no new high angle grain boundaries are created); (3) only a misorientation angle larger than 15° is classified as recrystallized. Recovered regions will therefore be registered as deformed material.

4.3. Effect of recovery

The hardness measurements show another course of annealing behaviour. The hardness value is proportional

to the flow stress of the material, which is strongly dependent on the dislocation density. This measurement should reflect both recovery and recrystallization effects. Determination of recrystallization kinetics from hardness measurements requires separation of the effects associated with concurrent recovery and recrystallization. Assuming that the isothermal recovery kinetics follow a logarithmic decay relationship, the time dependence of micro hardness is then given by the following expression [14, 15]

$$H_{\text{rec}} = A - B \ln t \tag{2}$$

Where H_{rec} is the hardness of an annealed sample if only recovery takes place, $A = H_1$, the hardness at 1 s annealing, and B, the slope of the straight line, as seen in Fig. 7a.

If the measured hardness, H, of the partially recrystallized materials follows the rule of mixtures it holds that

$$H = (1 - f)H_{\text{rec}} + f \cdot H_0 \tag{3}$$

Where f is the volume fraction of recrystallized grains. Assuming that the kinetics of concurrent recovery follow a straight line when recrystallization starts, by substituting Equation 2 into 3, the recrystallization fraction excluding prior and concurrent recovery can be as shown by the triangular symbols in Fig. 7b. If it is assumed that there is no concurrent recovery taking place after recrystallization starts, by setting $H_{\text{rec}} = 40.5$ the hardness at the start point of recrystallization (dotted line in Fig. 7a), one may exclude the prior recovery effect and obtain the recrystallized fraction only, as shown in Fig. 7b (square symbol). The recrystallized fraction with exclusion of only the prior recovery effect is about 10% higher than the value with exclusion of both prior and concurrent recovery effects. This also indicates that the concurrent recovery effects are significant during the early stages of recrystallization. By comparing the three curves in Fig. 7b, one can see that taking into account recovery is necessary to determine the recrystallization fraction. After subtraction of the recovery effect the resulting fraction recrystallized is in good agreement with the metallographic measurements, as shown in Fig. 8. The difference is within 5%.

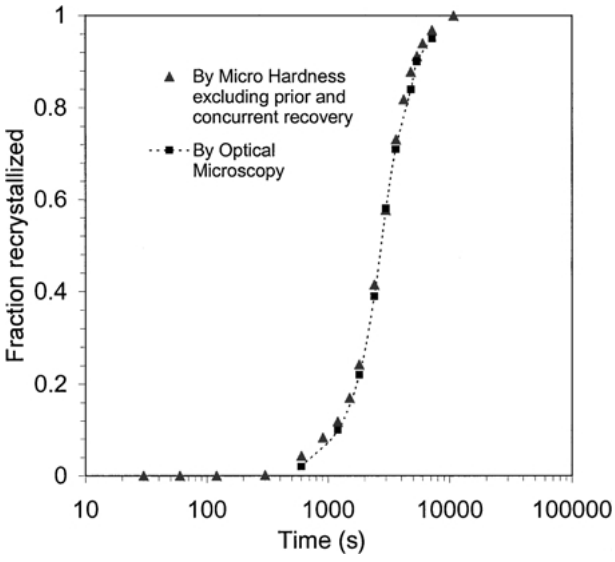

Figure 8 Comparison of fraction of recrystallized material quantified by micro-hardness tests and optical microscopy on the basis of the composite image method.

5. Conclusions

(1) A new method for characterizing the microstructure in AA1050 by optical microscopy is presented. Combining this method with an areal analysis technique yields a more accurate measurement of the fraction of recrystallized material, which is in excellent agreement with OIM measurements.

(2) Microhardness measurements demonstrate another course of annealing behaviour, which includes both effects associated with concurrent recovery and recrystallization processes. After subtraction of the effect of the concurrent recovery, the micro hardness test can provide a reasonable quantification of the recrystallized fraction developed with annealing time.

Acknowledgement

The authors thank E. Peekstok and P. Balke for assistance in optical microscopy and OIM, respectively.

References

1. E. C. W. PERRYMAN, *Trans. AIME, J. Metals* (1955) 1053.
2. P. L. ORSETTI ROSSI and C. M. SELLARS, *Acta. Mater.* **45** (1997) 137.
3. R. A. VANDERMEER, *Metal. Trans.* **1** (1970) 819.
4. P. FAIVRY and R. D. DOHERTY, *J. Mater. Sci.* **14** (1979) 897.
5. C. N. SPARKS, PhD thesis, University of Sheffield, 1993.
6. M. P. BLACK and R. L. HIGGINSON, *Scripta. Mater.* **41**(2) (1999) 125.
7. E. WOLDT and D. JUUL JENSEN, *Metall. Trans.* **26A** (1995) 1717.
8. O. ENGLER and G. GOTTSTEIN, *Steel Research* **63**(9) (1992) 413.
9. D. J. DINGLEY and K. BABA-KISHI, *Scanning Electron Microsc.* **27** (1986) 383.
10. T. FURU, R. ORSUND and E. NES, *Acta Met. Mater.* **43** (1995) 2209.
11. D. BOWEN, R. R. EGGLESTON and R. H. KROPSCHOT, *J. Appl. Physics.* **23**(6) (1952) 630.
12. K. MUKUNTHAN and E. B. HAWBOLT, *Metall. Mat. Trans. A* **27** (1996) 3410.
13. F. LI and P. S. BATE, *Acta Metall. Mater.* **39**(11) (1991) 2639.
14. F. J. HUMPHREYS and M. HATHERLY, "Recrystallisation and Related Annealing Phenomena" (Pergamon, London, 1996).
15. J. G. BYRNE, "Recovery, Recrystallization and Grain Growth" (MacMillan, New York, NY, 1965) 37.

Received 9 November 2000
and accepted 18 September 2001